A Phase Shifter Design For LCLS-II-HE

Zachary Wolf
Stanford Linear Accelerator Center

January 12, 2021

Abstract

This note presents a design for the LCLS-II-HE phase shifters. The design is similar to the LCLS-II phase shifters, but scaled to meet the new HE requirements.

1 Introduction[1]

The LCLS-II-HE project includes an upgrade to the LCLS-II SXR undulator line for 8 GeV operation. The SXR undulators will have a new period, and the SXR phase shifters must have a new larger phase integral. This note presents a magnetic design for the new phase shifters.

The LCLS-II SXR line used 20 phase shifters, and their structural parts will be reused for LCLS-II-HE. New magnet arrays will be added to the mechanical assemblies. In addition, 9 new phase shifter mechanical assemblies will be purchased and new magnet arrays will be added to them. LCLS-II-HE will have a total of 29 phase shifters.

The starting point for the LCLS-II-HE phase shifter magnetic design in this note will be the old LCLS-II SXR phase shifter magnetic design. It is a pure permanent magnet (PPM) structure designed to give no steering and no offset to the beam at any gap[2]. The design fixes the relative lengths of the magnet blocks, but the lengths of all the blocks can be scaled together, and the heights and widths of the blocks can be adjusted. In this note we find a set of block sizes that meets the LCLS-II-HE requirements.

The note starts by listing the physical constraints and phase shifter magnetic requirements. It then discusses why stronger phase shifters are required. It presents a computer model of the phase shifters and demonstrates that the model agrees with the measurements of the LCLS-II phase shifters. Using the model, it then presents a design that meets the LCLS-II-HE requirements. Phase shifter jumps are discussed, both during normal operation and during an energy scan. After that, the phase integral gap sensitivity and temperature sensitivity of the new design are discussed.

The note uses the convention that "z" is in the beam direction, "y" is up, and "x" makes a right handed system. Dimensions in the z-direction are called lengths; dimensions in the y-direction are called heights; and dimensions in the x-direction are called widths. This

[1]Work supported in part by the DOE Contract DE-AC02-76SF00515. This work was performed in support of the LCLS project at SLAC.

[2]Z. Wolf, "A PPM Phase Shifter Design", LCLS-TN-11-2, July, 2011.

naming scheme will be used extensively when discussing the phase shifter magnet block dimensions. In this case, the largest dimension will not be the "length" as one might intuit, but is rather the "width", so care is required. By block length, we always refer to the length of the longest block in the magnet array.

2 Space Constraints

The layout of the current SXR interspace region is shown in figure 1. The distance from

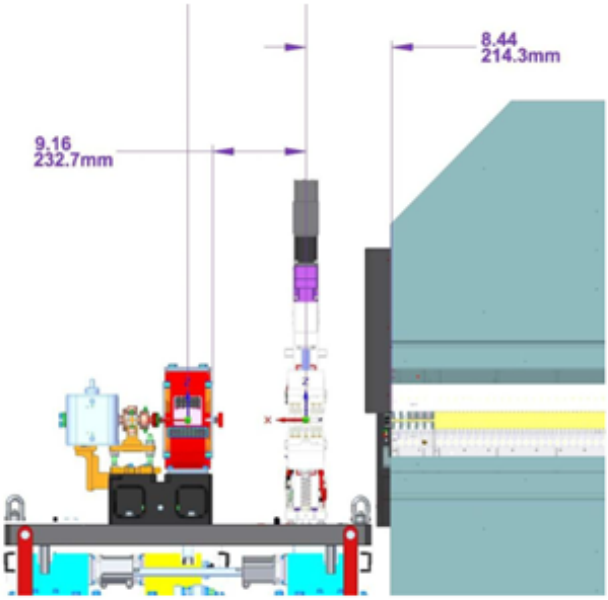

Figure 1: Interspace layout of the LCLS-II SXR line.

the quadrupole edge to the center of the phase shifter is 232.7 mm. The SXR phase shifter is 82.5 mm long in the beam direction. So the length from the edge of the quadrupole to the edge of the phase shifter is 232.7 mm - (1/2)82.5 mm = 191.45 mm.

The distance from the center of the phase shifter to the edge of the undulator is 214.3 mm. So the distance from the edge of the phase shifter on the quadrupole side to the edge of the undulator is 214.3 mm + (1/2)82.5 mm = 255.55 mm.

The SXR-HE line will have only small modifications to this layout. The SXR-HE undulators will have a pole extension at the ends of 7.5 mm. The distance from the edge of the phase shifter on the quadrupole side to the edge of the SXR-HE undulator is 255.55 mm - 7.5 mm = 248.05 mm. Because of a flange in the beam pipe, we wish for the dimension from the edge of the quadrupole to the edge of the phase shifter to not change. This is the reason that the edge of the phase shifter on the quadrupole side has been used as a reference. The SXR-HE dimensions are shown in figure 2.

The primary space constraint of interest to the magnetic design of the phase shifter is the length of the fringe fields since we need to avoid magnetic crosstalk to the quadrupole

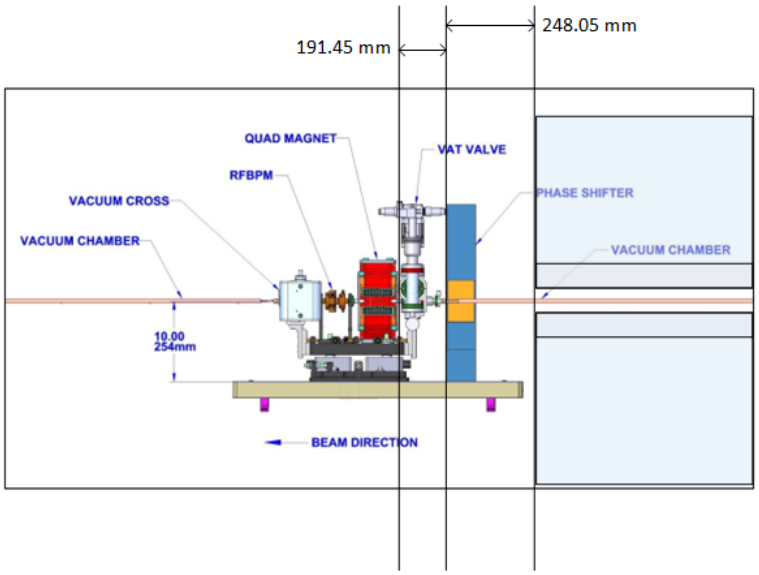

Figure 2: Interspace layout of the SXR-HE line. The dimensions show the distance from the edge of the phase shifter to the quadrupole and undulator.

and undulator. When designing the SXR-HE phase shifter, we have two primary space constraints. On the quadrupole side, the length of the fringe field must be less than 191.45 mm. On the undulator side, the length of the phase shifter plus the length of the fringe field must be less then 248.05 mm. The transverse dimensions of the magnet blocks do not have significant space constraints.

3 Requirements

The LCLS-II-HE phase shifter requirements come from a Physics Requirements Document[3]. The list of magnetic requirements are briefly summarized below. Additionally, some requirements not explicitly addressed in the Physics Requirements Document (PRD) are listed in order to complete the phase shifter specification.

The requirements below must be met for all gaps in the operating range. The field integral tolerances given below must be met for all horizontal and vertical positions within ±1.0 mm of the phase shifter beam axis. The phase integral tolerances must be met on the beam axis. To convert from phase to phase integral, the K values of the undulators must be used. The range of K is 1.51 to 9.21 for the SXR-HE undulators. The SXR-HE undulator period is 56 mm.

1. The gap operating range of the phase shifter is 10 to 35 mm.
2. The phase integral of the phase shifter at 10 mm gap must be larger than 9500 $\mathrm{T^2mm^3}$.
3. The phase change from the phase shifter must be accurate to 5.8° at all operational gap settings. Equivalently, the phase integral of the phase shifter must be accurate to 5.61 $\mathrm{T^2mm^3}$ (see section 10 for a derivation).
4. The change in phase integral in the range $x = \pm 0.30$ mm and $y = \pm 0.30$ mm must be less than 5.61 $\mathrm{T^2mm^3}$ in order for the phase shifter to remain within tolerance with fiducialization and alignment errors.
5. The first field integral of B_x and B_y must be within ±20 μTm. The second field integral of B_x and B_y must be within ±60 $\mu\mathrm{Tm}^2$.
6. The change in the first field integral due to neighboring devices must be less than 3 μTm. We use the 3 μTm change in first field integral to define the fringe field length.
7. The fringe field length must be less than 191.45 mm. The length of the phase shifter plus the length of the fringe field must be less than 248.05 mm.
8. There should be no phase shifter 2π phase jumps in a 10% energy scan.

[3] D. Cesar et al., "LCLS-II-HE SXR Undulator System", LCLS-II-HE Physics Requirements Document LCLSII-HE-1.3-PR-0049-R0, August, 2020.

4 The Need For A Stronger Phase Shifter

The LCLS-II SXR phase shifters were designed to have a modest phase integral in order to have modest gap accuracy and temperature accuracy requirements. The limited phase integral requires a number of 2π phase jumps in order to cover the range of K values of the undulators[4,5,6]. This is illustrated in figure 3 where the phase shifter is correcting the exit end of the upstream undulator and the entrance end of the downstream undulator. Details of the model used in the calculation and a comparison to experimental data are given in a technical note[7].

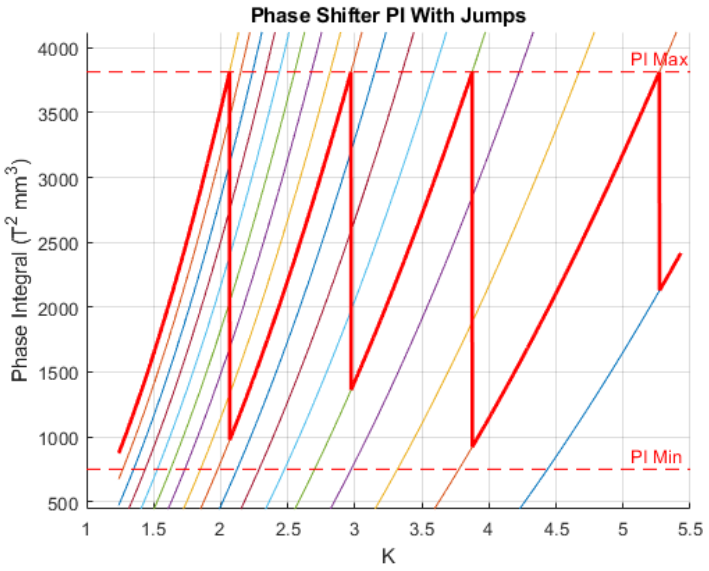

Figure 3: The LCLLS-II SXR phase shifters have a series of $2\pi n$ jumps to cover the range of undulator K values.

If an LCLS-II SXR phase shifter is used for the SXR-HE K range, the situation is that of figure 4. The phase shifter cannot stay within its phase integral range and cover the range of SXR-HE K values. The existing SXR phase shifters will not work for LCLS-II-HE and they need to be replaced.

If the phase integral range of the SXR-HE phase shifters is increased according to the LCLS-II-HE PRD, the phase shifters do cover the SXR-HE undulator K range as shown in figure 5. There are still jumps, but the phase shifters can operate as currently used in LCLS-II. This plot is only a rough illustration. The minimum phase integral at the maximum operating gap was not specified in the PRD, only the minimum phase integral

[4] Z. Wolf, "Setting The LCLS-II Phase Shifters", LCLS-TN-17-3-Rev2, February, 2018.

[5] Z. Wolf, Y. Levashov, H.-D. Nuhn., "Initial Tests Of Phase Matching An LCLS-II Undulator", LCLS-TN-18-1, February, 2018.

[6] Z. Wolf, Y. Levashov, "A Phase Matching Test Of The LCLS-II Undulators", LCLS-TN-19-5, November, 2019.

[7] Z. Wolf, Y. Levashov, H.-D. Nuhn, "Initial Tests Of Phase Matching An LCLS-II Undulator", LCLS-TN-18-1, February, 2018.

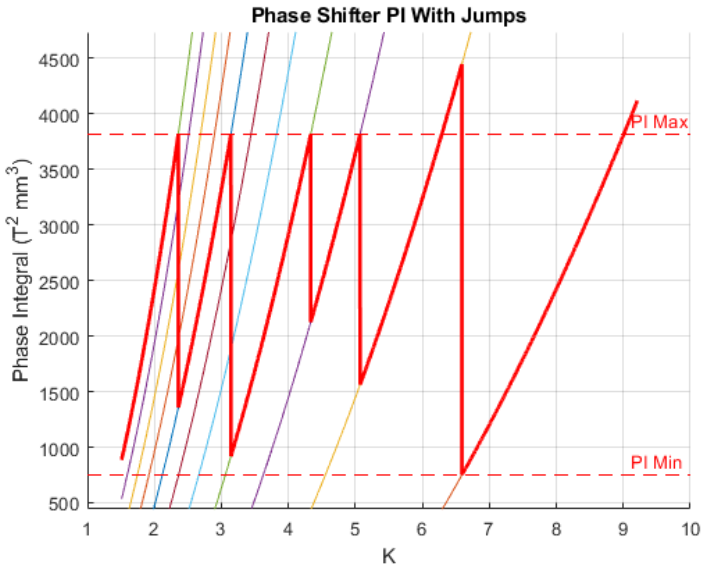

Figure 4: An LCLS-II SXR phase shifter can not be used to cover the range of K values of LCLS-II-HE.

used in the PRD calculations. The SXR-HE phase shifter jumps will be discussed in detail below once the phase integral range of the designed phase shifter is known.

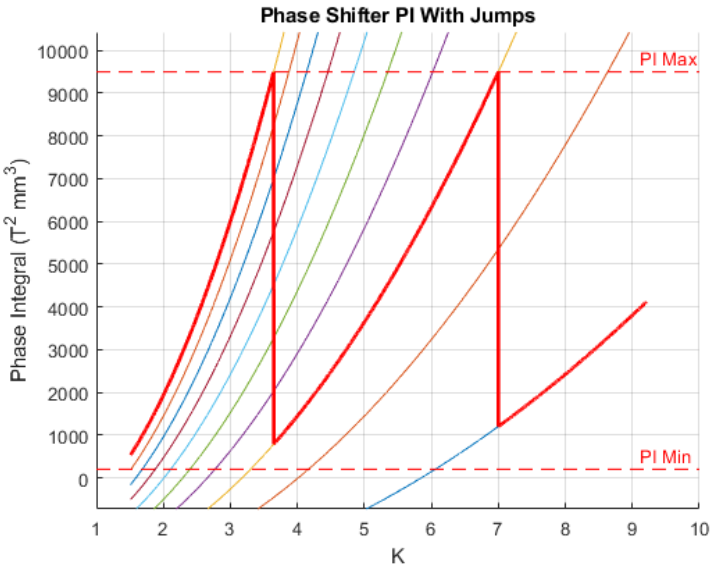

Figure 5: The proposed LCLS-II-HE phase shifters cover the range of undulator K values.

5 Phase Shifter Model

In order to proceed to make a phase shifter magnetic design that meets the requirements listed above, we must make a model that gives the phase integral, fringe field length, and other necessary quantities as a function of the magnet array parameters. We use the same approach used for the LCLS-II SXR magnet structure. The magnet array is modelled as a set of magnetic charges as detailed in a technical note[8]. In this section we verify the model by comparing its output to LCLS-II SXR phase shifter measurements.

Figure 6 illustrates the charge model. The magnet blocks are replaced by magnetic charges on their surfaces. The size of the blocks, their remnant field, and the gap are input parameters to the model.

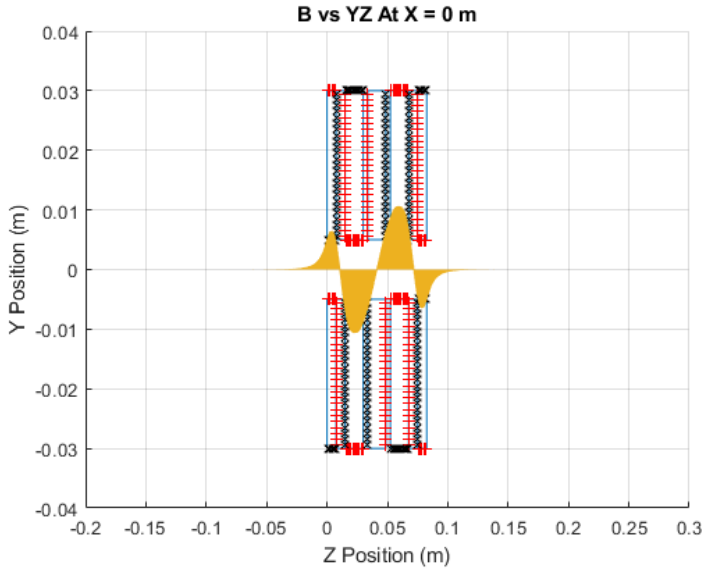

Figure 6: Model of the phase shifter in which the magnet blocks are replaced by magnetic charges.

A plot of phase integral as a function of gap for both a measured phase shifter, SXPS-16336, and the model of an SXR phase shifter is shown in figure 7. The agreement is very good. The model uses the datasheet "typical" value of $B_r = 1.25$ T for the VACODYM 983 TP magnet material. The blocks in the model have length 15 mm, height 25 mm, and width 65 mm, the same as the SXR phase shifters. The gap in the model has a free parameter that was used in the comparison. The gap of the actual phase shifter is set by opening the gap until a 10 mm gauge block freely goes through it. At that point, the encoder offset is adjusted so the gap reads 10 mm. This is done after the blocks have been moved to tune the phase shifter, so the gap is actually larger than the smallest gap in the phase shifter. In order to make the model agree with the measurements, the modeled gap had to be increased by 600 μm. This is a reasonable value considering how the actual phase

[8] Z. Wolf, "A PPM Phase Shifter Design", LCLS-TN-11-2, July, 2011.

shifter gap is set. The phase shifter design should be a little stronger than the requirement to account for the actual gap being larger than the modeled gap.

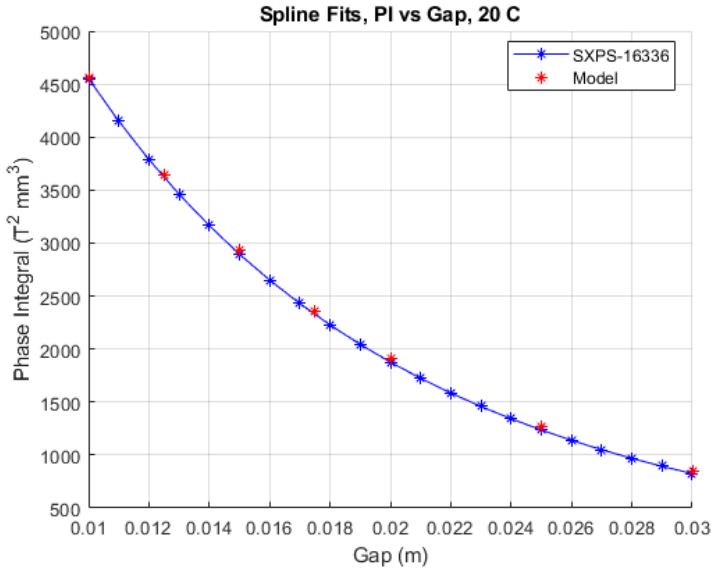

Figure 7: Phase integral as a function of gap for a measured phase shifter and the model.

Another check on the model is whether it gets the fringe fields correct. Figure 8 shows the length of the fringe fields of SXPS-16336 and the model. The length of the fringe field is defined to be the distance from the end of the magnet blocks to the point after which the first field integral changes by less than 3 μTm. The agreement of the measurements and the model is reasonably good. The measurements have some error because small offsets in the probe have a large effect on the fringe field length. In general, however, the model gives a reasonable estimate of the fringe field length.

The idea behind the fringe field limit is that if a steel object is placed in the fringe field and truncates the field on the beam axis, the field integral will change by less than 3 μTm compared to its value measured in the lab. This allows the lab measurements, which are done without nearby steel objects, to be used in the tunnel making only small errors. It minimizes the effect of combined undulator and phase shifter gap dependent field integral changes.

The magnetic crosstalk was measured between all neighboring devices in LCLS-II. Figure 9 shows the change in the first integral of B_y as the phase shifter was brought closer to the undulator[9]. (Prototype devices were actually used.) The phase shifter gap was 40 mm and the undulator gap was 7.2, 10, and 20 mm for the three datasets in the figure. The first integral changes by 3 μTm compared to large separation when the undulator and phase shifter are about 130 mm apart. This agrees well with the model and the calculated fringe field length for SXPS-16336 at 40 mm gap.

In summary, the charge model does a good job of agreeing with the actual phase shifter

[9] S. Anderson, "Undulator Interspace Component Spacing Tests", LCLSII-3.2-EN-0358-R0, January, 2015.

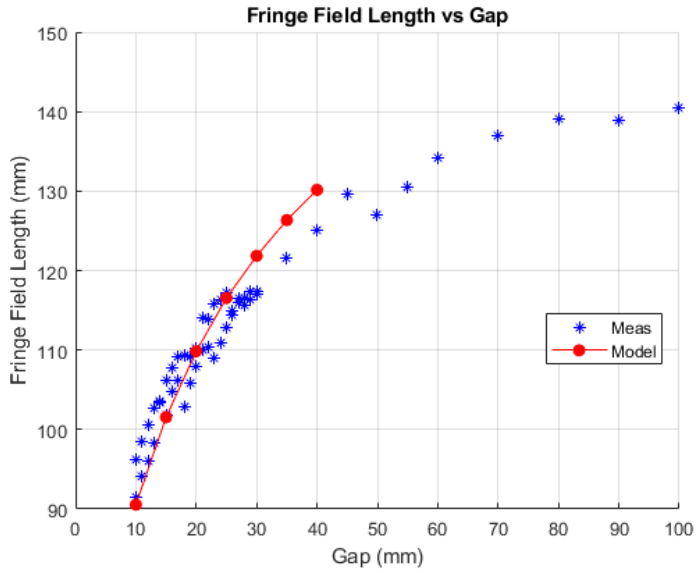

Figure 8: Length of the fringe field from SXPS-16336 and from the model.

measurements. We use the charge model to design the magnet array in the sections below. After the design is complete, we must build a prototype to confirm that the magnet design meets the requirements.

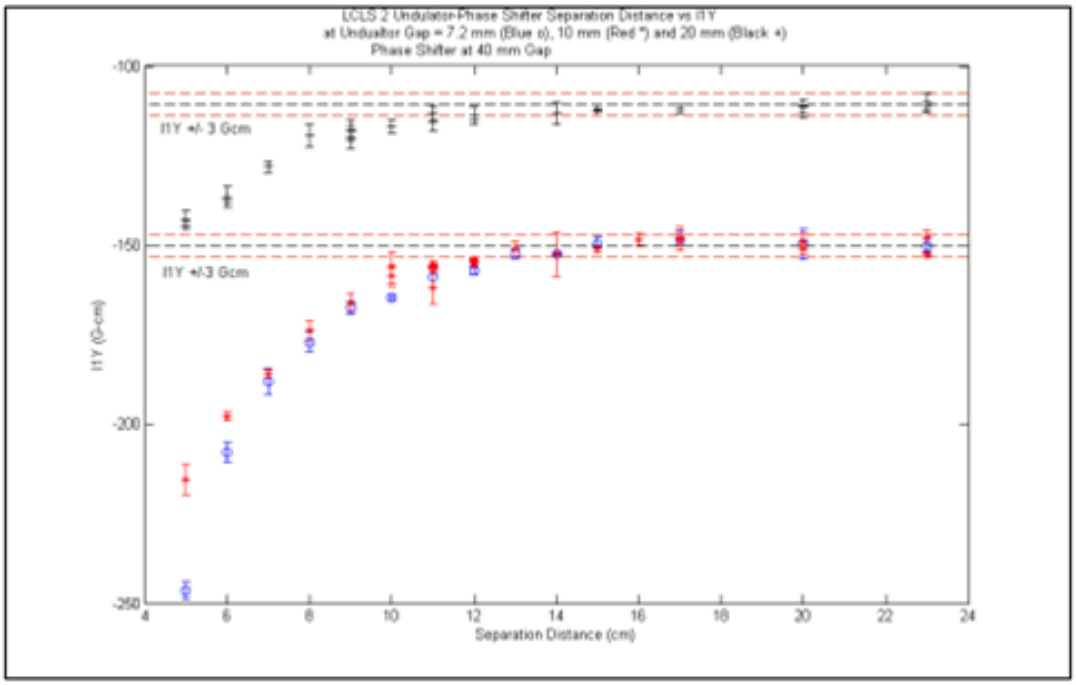

Figure 9: Measured magnetic crosstalk between an LCLS-II undulator and phase shifter.

6 Phase Shifter Magnetic Design

6.1 Phase Integral Study

For the phase shifter magnetic design, we first study how the phase integral depends on the magnet block dimensions. We expect the phase integral to depend most strongly on the block length since the field increases with block length and each of the integrals in the phase integral definition increases with block length. We also expect the phase integral to increase with block height since moving the opposite charges on the tops of the upper blocks and bottoms of the lower blocks to distances even further away from the beam axis should make the field larger on the axis. This effect depends on the block height and should diminish at large heights. A similar argument applies to the width of the blocks. Adding magnetic material at some width increases the field, but the effect diminishes at large width. We expect to meet the phase integral requirement primarily by adjusting the block length, but the block height and width can also be used, and each dimension's effect on the fringe field must be considered.

We start with the LCLS-II SXR phase shifter dimensions and make small changes. In this way we linearize the problem. We find the sensitivity of the phase integral to block length, height, and width.

Figure 10 shows the modeled phase integral as a function of block length at 10 mm gap. The block height is 25 mm and the block width is 65 mm, the same as the SXR phase shifters. The block length of the SXR phase shifters is 15 mm. A linear fit to the phase integral over the small range of block lengths gives a sensitivity of

$$\frac{dPI}{dL_b} = 1446 \text{ T}^2\text{mm}^3/\text{mm}$$

From the figure, a phase integral of 9500 T^2mm^3 requires a block length of approximately 18.5 mm. As noted above, when setting the encoder offset, we give up some of the gap when we require a 10 mm gauge block to slide through. We choose a block length of 19 mm which gives a phase integral over $10,000$ T^2mm^3.

If we convert from block length to phase shifter length, we get the plot in figure 11. A block length of 19 mm gives a phase shifter length of 104.5 mm. The conversion factor from block length to phase shifter length is 5.5 and a plot of phase shifter length vs block length is shown in figure 12.

The sensitivity of the phase integral to block height is shown in figure 13. The gap is 10 mm. The block length is 19 mm and the block width is 65 mm. The sensitivity of phase integral to block height is

$$\frac{dPI}{dH_b} = 265 \text{ T}^2\text{mm}^3/\text{mm}$$

This is a factor of 5 smaller than the sensitivity to block length.

Figure 14 shows the dependence of phase integral to block width. The gap is 10 mm. The block length is 19 mm and the block height is 25 mm. The sensitivity of the phase integral to block width is

$$\frac{dPI}{dW_b} = 13 \text{ T}^2\text{mm}^3/\text{mm}$$

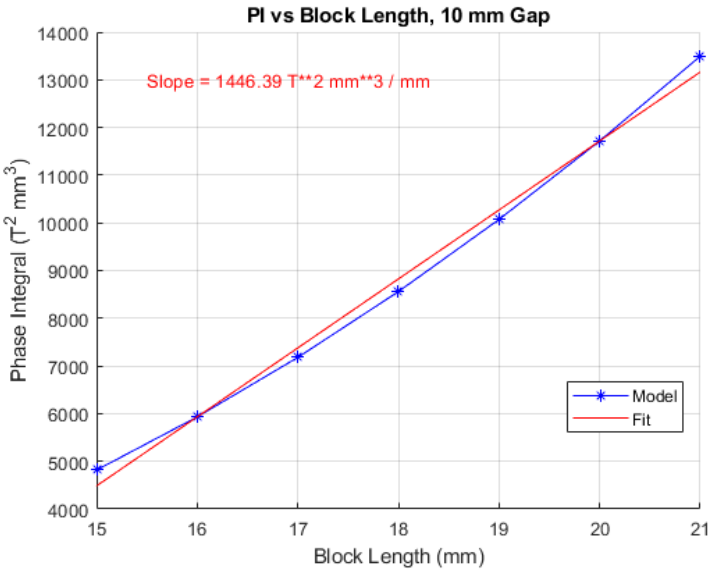

Figure 10: Phase integral as a function of block length at 10 mm gap. The block height is 25 mm and the block width is 65 mm.

The sensitivity is small, but it is a way to increase the phase integral without increasing the fringe field length, as we will see below.

We now take the block length to be 19 mm. After the fringe field is studied, adjustments can be made. A block length of 19 mm gives a phase shifter length of 104.5 mm. Since the maximum length of the phase shifter plus the fringe field is 248.05 mm, the maximum fringe field length with 19 mm blocks is 143.55 mm. This is below the 191.45 mm fringe field length allowed on the quadrupole side and it gives the tighter constraint.

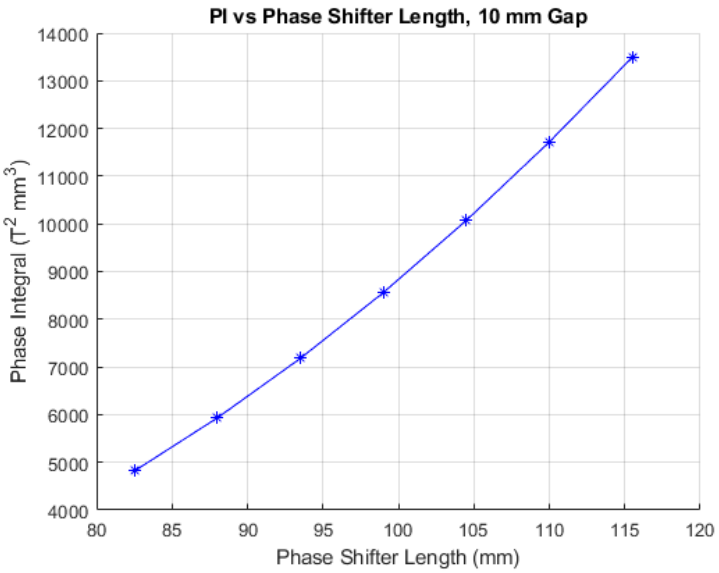

Figure 11: Phase integral as a function of phase shifter length.

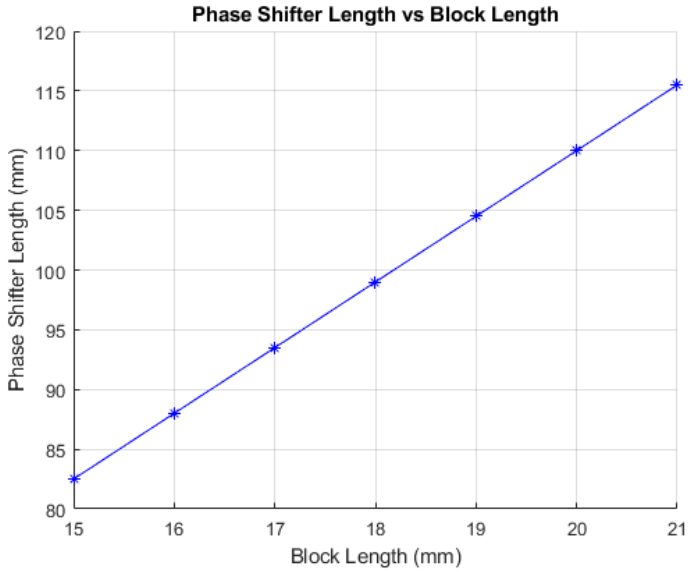

Figure 12: Phase shifter length as a function of block length.

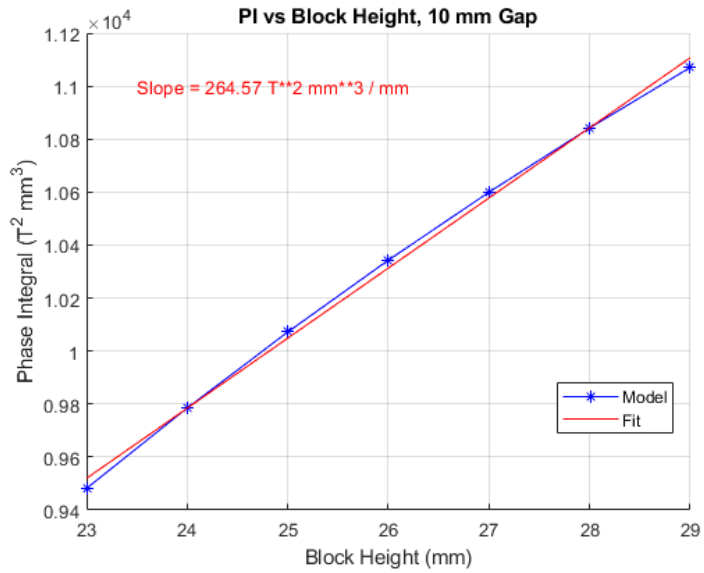

Figure 13: Phase ingegral as a function of block height at 10 mm gap. The block length is 19 mm and the block width is 65 mm.

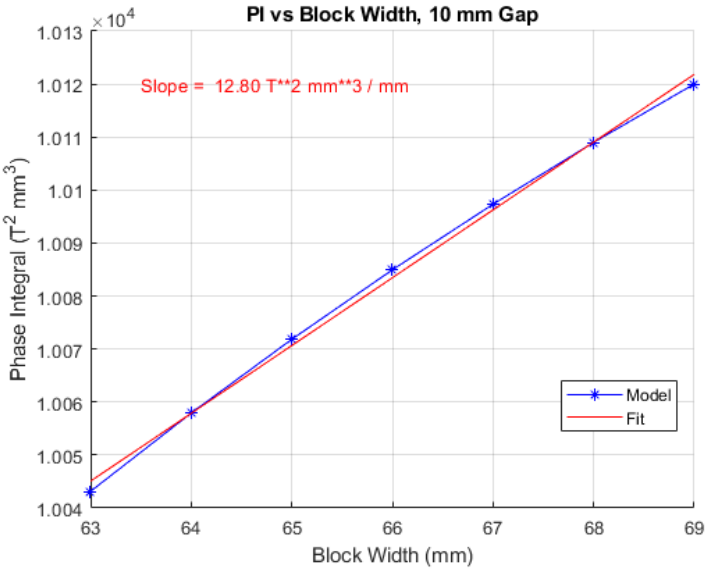

Figure 14: Phase integral as a function of block width at 10 mm gap. The block length is 19 mm and the block height is 25 mm.

6.2 Fringe Field Study

The fringe field length depends strongly on gap. The gap dependence is shown in figure 15. The figure is for blocks 19 mm long, 25 mm high, and 65 mm wide. In order to study the fringe field, we set the gap to the maximum operating gap in the PRD, 35 mm.

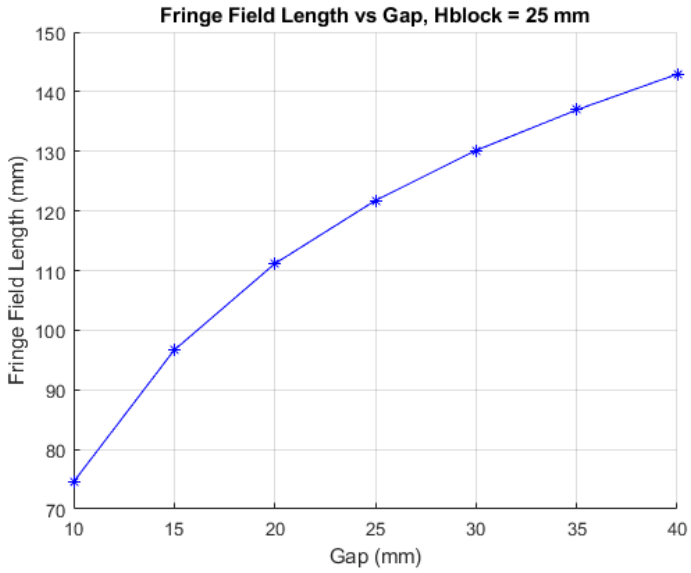

Figure 15: Fringe field length as a function of phase shifter gap.

We first study how the fringe field length depends on the length of the blocks. There is a length dependence because longer blocks move the magnetic charges further apart making larger fields at a distance. The dependence of fringe field length on block length is shown in figure 16. The dependence over the length range has a small non-linear component, but a line is fit in order to compare with the sensitivity to block height. The sensitivity of the fringe field length to the block length is

$$\frac{dL_{ff}}{dL_b} = 1.66 \text{ mm/mm}$$

The phase shifter length is 5.5 times the block length, so the total length of the phase shifter and fringe field on one side is

$$\begin{aligned} L_{ps\_ff} &= 5.5L_b + 1.66L_b \\ &= 7.16L_b \end{aligned}$$

Increasing the block length by 1 mm increases the phase shifter plus fringe field length by about 7.2 mm. This will put a strong limit on how long the blocks can be.

We expect the fringe field length to depend strongly on block height. This is again because moving the magnetic charges further apart makes the fields larger at a distance. The fringe field length as a function of block height is shown in figure 17. The block length

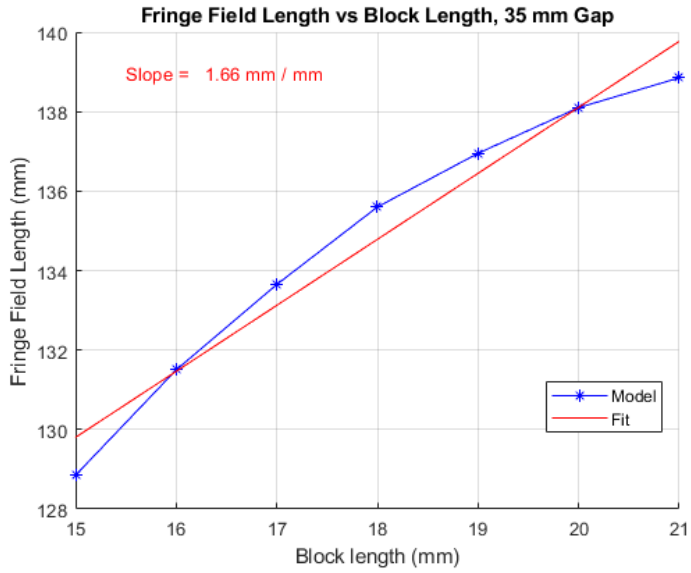

Figure 16: The fringe field length depends on the block length.

is 19 mm, the block width is 65 mm, and the gap is 35 mm. The sensitivity of the fringe field length to the block height is

$$\frac{dL_{ff}}{dH_b} = 2.49 \text{ mm/mm}$$

For a block height of 25 mm, the fringe field length is 137 mm. The limit is 143.6 mm. In theory, with a sensitivity of 2.49 mm/mm, the block height could be increased to 27 mm, but that would use up the entire budget and leave no room for errors. We keep the block height at 25 mm.

The dependence of fringe field length on block width is expected to be negligible. It is very small, as shown in figure 18. The sensitivity of fringe field length to block width is

$$\frac{dL_{ff}}{dW_b} = 0.46 \text{ mm/mm}$$

In summary, the requirements on phase integral and fringe field length are met with a block length of 19 mm, a block height of 25 mm, and a block width of 65 mm. In theory the block length could be increased by 0.9 mm, or the block height could be increased by 2 mm. This would use up the entire fringe field length budget leaving no room for modeling errors or positioning errors. We choose not to do this.

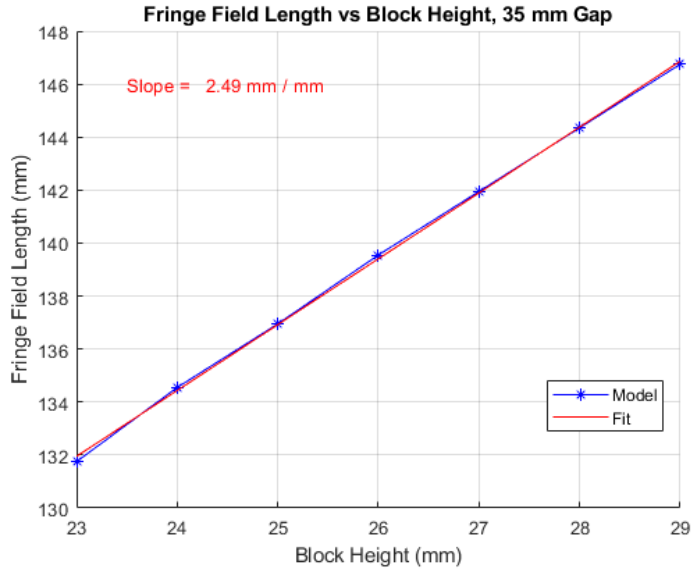

Figure 17: Fringe field length as a function of block height.

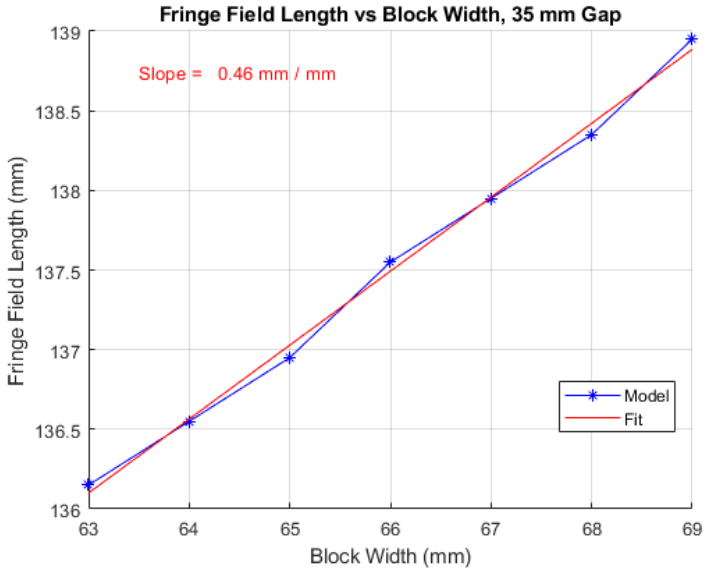

Figure 18: Fringe field length as a function of block width.

6.3 Field Uniformity Study

With a block length of 19 mm, a block height of 25 mm, and a block width of 65 mm, the phase integral as a function of x is shown in figure 19, and the phase integral as a function of y is shown in figure 20. In both plots the gap is 10 mm. The dashed lines are at a phase integral difference limit of 5.6 T^2mm^3 from the value on the axis. The phase integral will be within tolerance if its axis is placed within approximately ± 1.8 mm in x and ± 0.3 mm in y of the beam axis. The tightest limit is at 10 mm gap, and the placement tolerance is relaxed at larger gaps. The ± 0.3 mm tolerance in y sets the fiducialization plus alignment tolerance of the phase shifter.

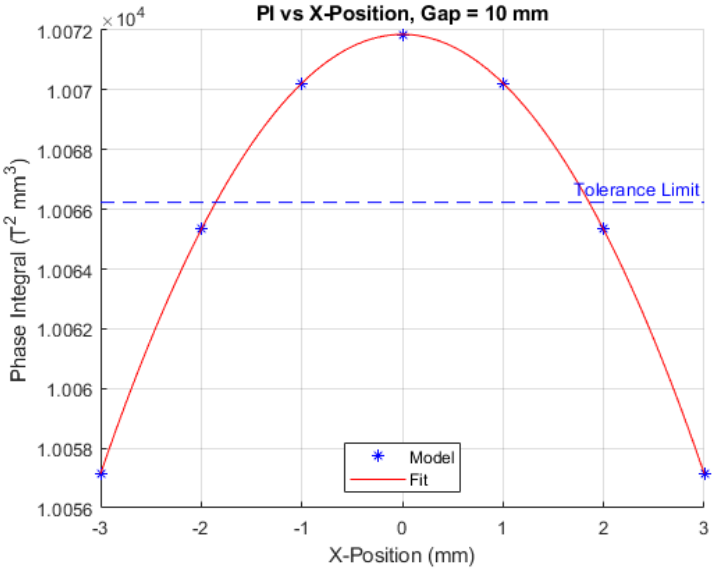

Figure 19: Phase integral as a function of x with $y = 0$.

The placement tolerance in x is large, and one might consider reducing the width of the magnet blocks. If the block widths are reduced to 50 mm, the phase integral is reduced to 9742 T^2mm^3. The block length would need to be increased by 0.25 mm to get back to $10,000$ T^2mm^3. The phase shifter length would increase by 1.38 mm, and the phase shifter plus fringe field length would increase by 2 mm. This would use up 2 mm of the 6 mm fringe field length surplus. If the phase shifter frame can withstand the increased magnetic forces, it does not seem prudent to reduce the magnet block widths and push the design so close to the tolerance limits.

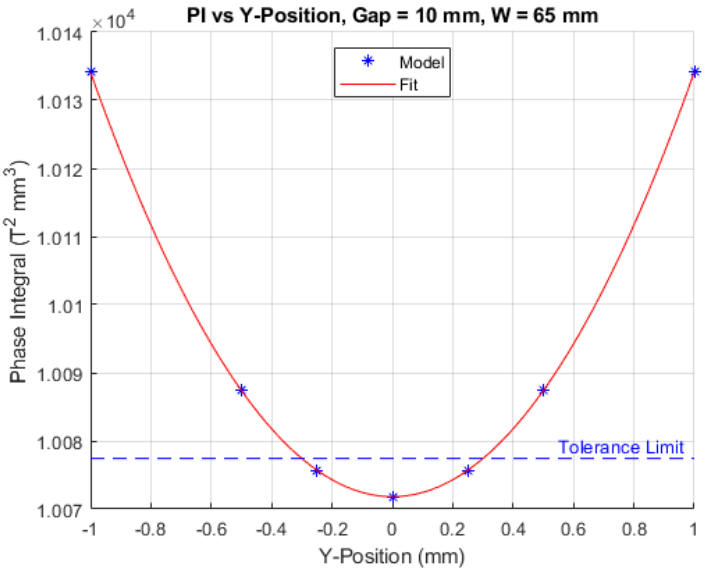

Figure 20: Phase integral as a function of y with $x = 0$.

6.4 Magnetic Design Summary

In the model we assumed $B_r = 1.25$ T. This is the remnant field of VACODYM 983 TP magnet material which was used for the SXR phase shifters. The requirements on phase integral and fringe field length are met with a block length of 19 mm, a block height of 25 mm, and a block width of 65 mm. The phase integral as a function of gap is shown in figure 21. The phase integral at 10 mm gap is $10,072$ T^{2}mm^3. The fringe field length as a function of gap is shown in figure 22. The ± 0.3 mm vertical region where the phase integral is within tolerance is adequate to accommodate reasonable fiducialization and alignment errors.

A check of these results was made using Radia[10]. With no magnet block permeability, the same as the charge model of this note, the phase integral at 10 mm gap was $10,067$ T^{2}mm^3. This is very close to the result from the charge model given above. When the permeability of the NeFeB magnet material was added in Radia, the phase integral at 10 mm gap was reduced to 9734 T^{2}mm^3. This is still above the required value of 9500 T^{2}mm^3, but is closer to the limit.

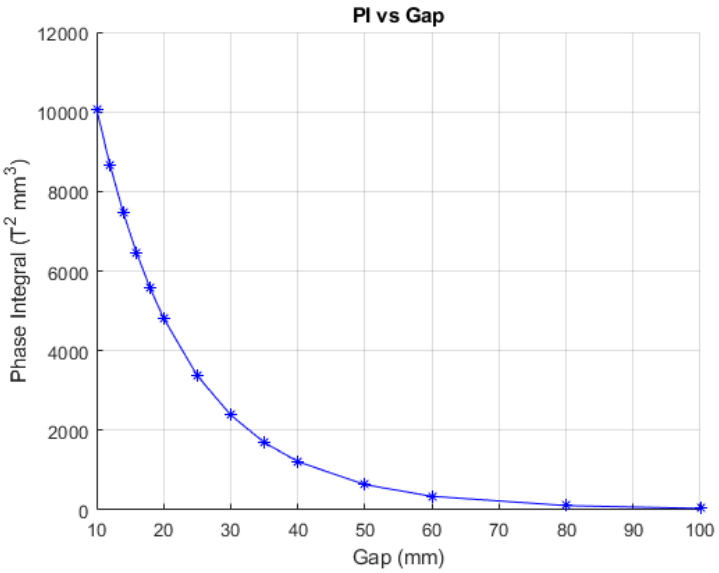

Figure 21: Phase integral as a function of gap.

The phase integral at 35 mm gap is 1693.5 T^{2}mm^3. We will use this as the minimum phase integral in the operating range of the phase shifter. Increasing the gap past 35 mm will exceed the limit on the fringe field length, so making the minimum phase integral in the operating range smaller is not possible. The minimum phase integral affects the number of phase shifter jumps over the K range of the undulators, as we will see in the next section.

[10] Heinz-Dieter Nuhn, private communication.

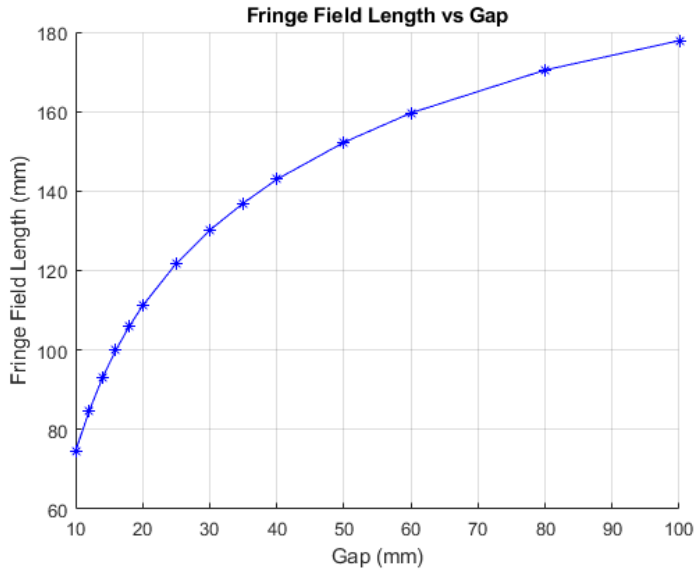

Figure 22: Fringe field length as a function of gap.

7 Phase Shifter Jumps

The 2π phase jumps required to cover the undulator K range was briefly discussed in a previous section. Now that the minimum phase integral of the operating range is known, we can better estimate the required jumps. We take the operating phase integral range of the phase shifter to be 1693.5 T^2mm^3 at 35 mm gap to 9500 T^2mm^3 at 10 mm gap. The maximum phase integral is reduced from the modeled value to account for setting the encoder offset, as must be done in practice. With this phase integral range, the jumps for a standard phase shifter with an undulator in each neighboring cell are shown in figure 23.

The phase shifter in front of the self-seeding cell must correct for the longer drift length of the cell. The jumps for this cell are shown in figure 24. The jump behavior of both a standard cell and the self-seeding cell is very similar to the case in LCLS-II.

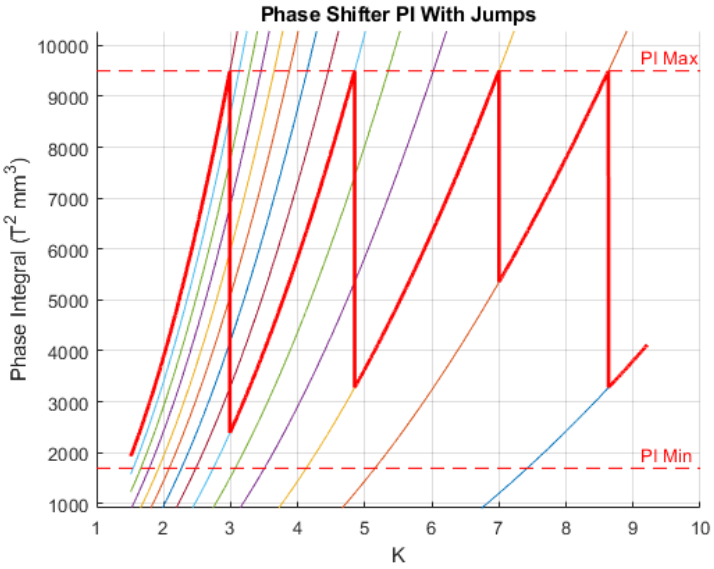

Figure 23: Phase shifter jumps for an interspace with an undulator in each neighboring cell.

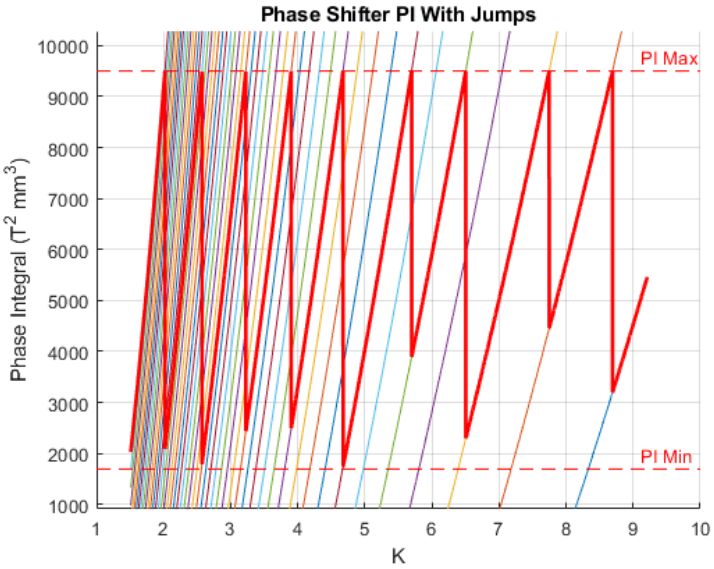

Figure 24: Phase shifter jumps when correcting for the drift in a cell without an undulator.

8 Energy Scan

An energy scan should not have jumps because they take extra time to change the phase shifter gap. An algorithm to avoid jumps during a scan is to set the minimum phase integral to a higher value and use the lowest photon energy of the scan (highest K value of the scan) to determine the multiple of 2π to add to the phase correction. For other K values in the scan (as K is decreased), the multiple of 2π is kept constant. The phase integrals can go lower than what the jump algorithm initially gave, as long as they stay above the minimum phase integral. This is illustrated in figure 25 for a 10% photon energy scan of an SXR-HE phase shifter. As the figure shows, the requirement specified in the PRD of a 10% photon energy scan without jumps can be met with the phase shifter design of this note.

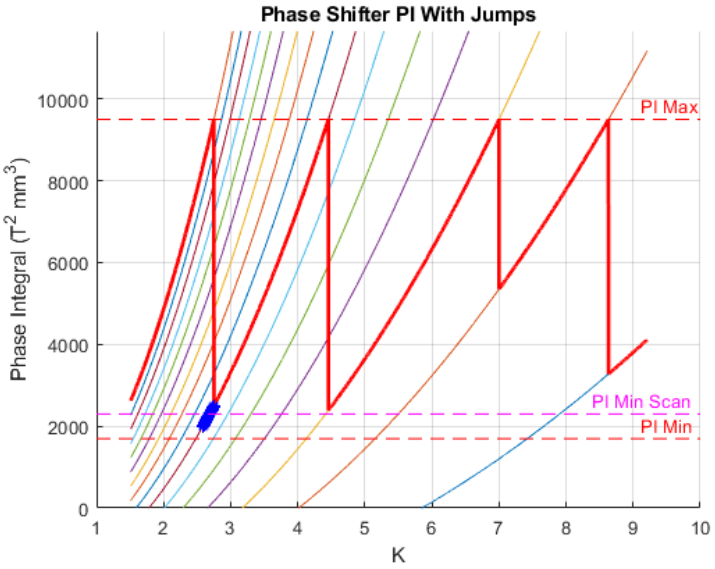

Figure 25: During an energy scan, the phase integrals can follow a curve with a given additive multiple of 2π. The minimum phase integral setting for the scan keeps the phase integral larger than the actual minimum.

The same algorithm described above works with the SXR-HE phase shifters correcting a cell without an undulator as illustrated in figure 26 for a 10% photon energy scan. The operational minimum phase integral limit must be increased for the scan, but the phase integral can stay within the phase shifter range during the scan.

We conclude that a phase shifter that meets the maximum phase integral requirement of the PRD and with the minimum operational phase integral from the design in this note can perform 10% energy scans with no jumps.

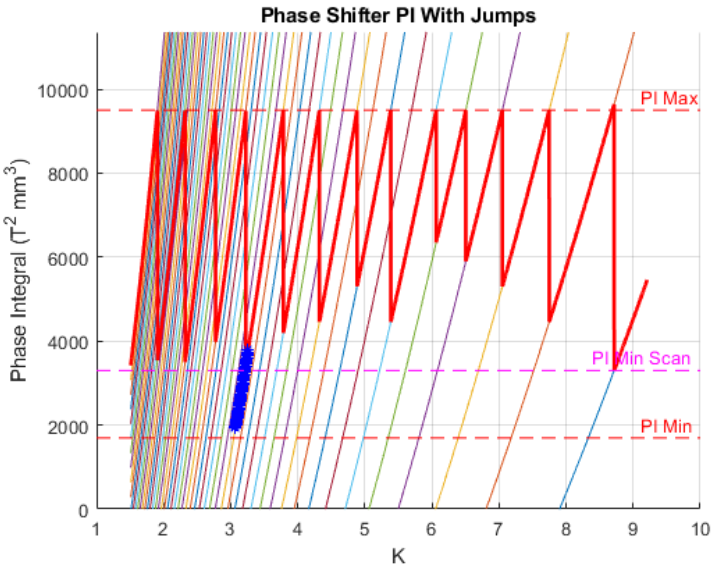

Figure 26: Phase shifter settings during a 10% energy scan for a cell with no undulator.

9 Magnetic Forces

We calculate the force on a phase shifter jaw by integrating the stress tensor over a surface encompassing the jaw.

$$\begin{aligned} F_i &= \iint \sigma_{ij} dS_j \\ &= \iint \left(\frac{1}{\mu_0} B_i B_j - \frac{1}{2\mu_0} B^2 \delta_{ij} \right) dS_j \end{aligned}$$

If we take the surface to include the midplane of the phase shifter and an enclosing surface far away, we calculate the vertical force on a jaw by integrating over the midplane

$$\begin{aligned} F_y &= \iint \sigma_{yy} dx dz \\ &= \iint \frac{1}{2\mu_0} \left(B_y^2 - B_x^2 - B_z^2 \right) dx dz \end{aligned}$$

B_x and B_z vanish on the midplane because of the top to bottom antisymmetry of the device, so

$$F_y = \iint \frac{1}{2\mu_0} B_y^2 dx dz$$

We approximate the integral by first integrating in the x-direction and replacing the integral by a constant effective width of the field times the field on the magnetic axis.

$$F_y = \frac{1}{2\mu_0} W_{eff} \int B_y^2 dz$$

where the integral is taken along z at $x = 0$, $y = 0$. The effective width of the field is given by

$$W_{eff} = \frac{\int B_y^2 dx}{\max(B_y^2)}$$

In the calculation below, we do the integral in x at a z-location where B_y is maximum. Using the model of the phase shifter, we proceed to calculate W_{eff} and $\int B_y^2 dz$ on the magnetic axis.

At 10 mm gap, the field B_y as a function of z at $x = 0$, $y = 0$ is shown in figure 27. The plot looks similar at other gaps, but the field is reduced.

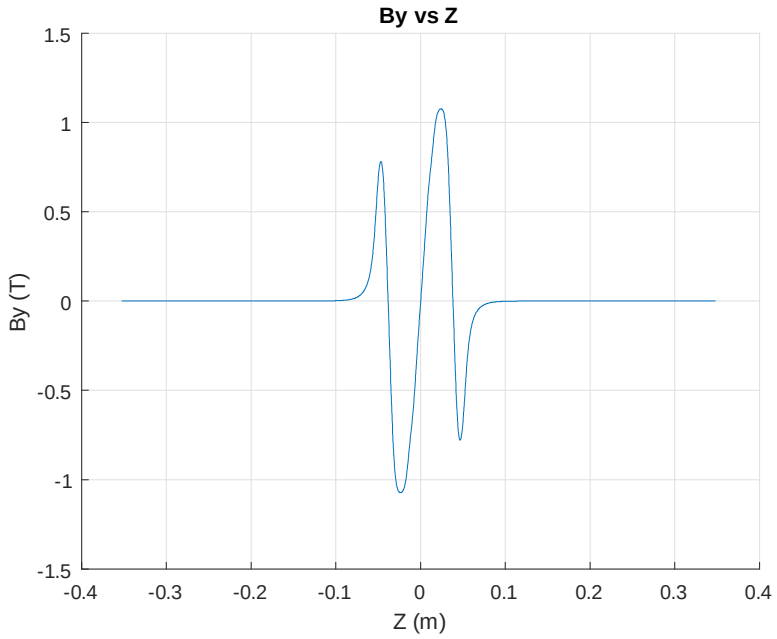

Figure 27: The vertical field B_y as a function of z on the magnetic axis with 10 mm gap.

At a field peak along z, the field B_y as a function of x at several gaps is shown in figure 28. When the field is squared and integrated in x, and then divided by the square of the peak field, the effective width is obtained as shown in figure 29.

In order to estimate the force, we set the effective width of the field to a constant value of 57 mm. We took the full field at each gap without making an allowance for setting the encoder offset. In this case, the estimated force on a jaw as a function of gap is shown in figure 30. At 10 mm gap, the force is about 1379 N, or 310 pounds.

When the same analysis is performed on an SXR phase shifter, the effective width of the field at 10 mm gap is again 57 mm and the calculated vertical force on a jaw at 10 mm gap is 962 N, or 216 pounds. In order to reach a force of 310 pounds, the gap must be closed to 7.0 mm. The effect of the larger SXR-HE force on the existing SXR phase shifter structure can be studied in this way by reducing the gap to 7.0 mm using the existing SXR magnet array. A mechanical analysis should also be performed to study how the increased force

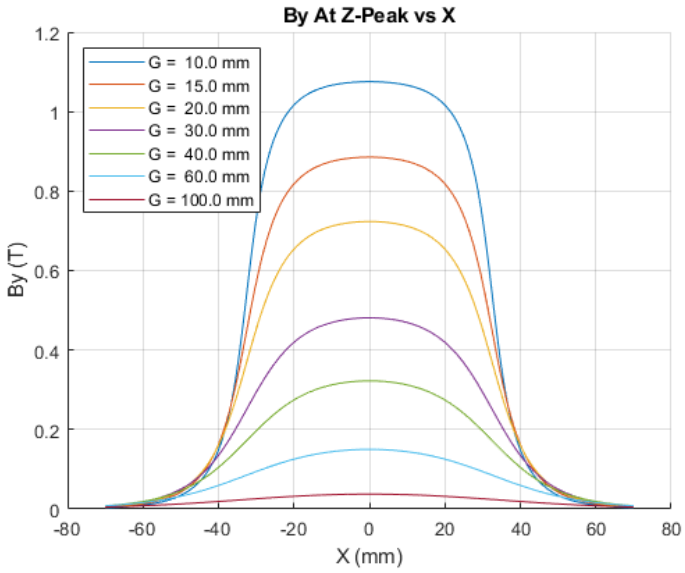

Figure 28: Field B_y as a function of x at several gaps at a z-position where the field is maximal.

from the SXR-HE magnet structure affects the structural frame of the SXR phase shifters, which will be reused for SXR-HE. The mechanical analysis can be compared to an SXR phase shifter at 7 mm gap.

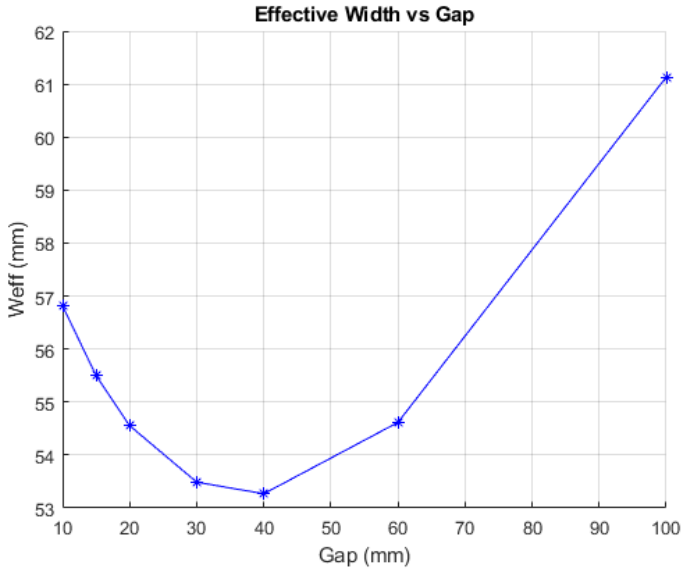

Figure 29: Phase shifter effective width as a function of gap.

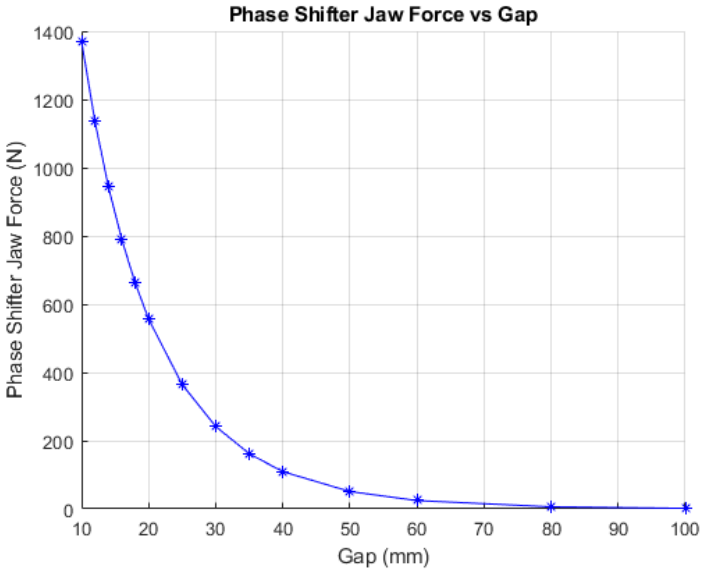

Figure 30: Force on a phase shifter jaw as a function of gap.

10 Gap Tolerance

Assuming only a vertical field, the slippage through the phase shifter is given by

$$S(z) = \int \left(\frac{1}{2} \frac{1}{\gamma^2} + \frac{1}{2} x'^2 \right) dz$$

The trajectory slope is given by

$$x'(z) = -\frac{q}{\gamma m v_z} \int B_y(z)\, dz$$

Inserting this formula for x' into the slippage equation and considering only the added slippage from the field gives

$$S(z) = \int \left(\frac{1}{2} \left[-\frac{q}{\gamma m v_z} \int B_y(z')\, dz' \right]^2 \right) dz$$

We define the phase integral PI as

$$PI = \int \left(\int B_y(z')\, dz' \right)^2 dz$$

In terms of the phase integral, the slippage in the phase shifter assuming $v_z = c$ is

$$S = \frac{1}{2\gamma^2} \left(\frac{q}{mc} \right)^2 PI$$

To find the phase change in the phase shifter ϕ, we multiply the slippage by $2\pi/\lambda_r$. Expressing λ_r in terms of the undulator period and K value, we find

$$\phi = 2\pi \frac{\left(\frac{q}{mc} \right)^2 PI}{\lambda_u \left(1 + \frac{1}{2} K^2 \right)}$$

If there is an error in the phase integral dPI, the error in the phase is

$$d\phi = 2\pi \frac{\left(\frac{q}{mc} \right)^2}{\lambda_u \left(1 + \frac{1}{2} K^2 \right)} dPI$$

The tolerance on the error in the phase as given in the PRD is

$$d\phi = 5.8 \text{ deg}$$

The undulator period is $\lambda_u = 56$ mm and the minimum operational K value is 1.51. This gives a limit on dPI of

$$dPI = 5.61 \text{ T}^2\text{mm}^3$$

The change in phase integral with gap is maximal at small gap and from the model is approximately

$$\frac{dPI}{dg} = -705 \text{ T}^2\text{mm}^3/\text{mm}$$

This gives a gap tolerance of

$$dg = dPI/(dPI/dg)$$

Inserting the values for dPI and dPI/dg, we get

$$dg = 8\ \mu\text{m}$$

If the phase shifter is well built, this should not be a difficult tolerance to meet.

11 Temperature Tolerance

From the previous section, the phase integral must be known to

$$dPI = 5.61\ \text{T}^2\text{mm}^3$$

The SXR phase shifters had a temperature calibration performed[11]. It was found that the phase integral temperature dependence is almost entirely due to the temperature dependence of the magnetic material. We found

$$\frac{1}{PI}\frac{dPI}{dT} = -1.64 \times 10^{-3}\ 1/\text{deg C}$$

The temperature error limit is given by

$$dT = \frac{dPI}{PI} \Big/ \left(\frac{1}{PI}\frac{dPI}{dT}\right)$$

Using $PI = 9500\ \text{T}^2\text{mm}^3$, we find

$$dT = 0.36\ \text{deg C}$$

In general, measuring the temperature of the phase shifter to this accuracy is not a problem. The SXR phase shifters, however, have a design problem in that the encoder read head is mounted on the bottom jaw. This heats the bottom jaw as shown in figure 31. The figure shows for each phase shifter two measurements of both the top and bottom jaw taken during the phase shifter calibrations. The temperature of the bottom jaw is about 0.3 deg C higher than the top jaw.

We wish to use a single phase shifter temperature when performing temperature corrections in the tunnel. The simplest method is to measure both the top and bottom jaws and average, as was done for LCLS-II. With the temperature difference between jaws about equal to the temperature tolerance, it is important that the same method to specify temperature must be used to determine the temperature in the tunnel as used when doing the temperature calibrations.

[11] Z. Wolf, Y. Levashov, "Temperature Dependence of the LCLS-II Undulators and Phase Shifters", LCLS-TN-20-1, April, 2020.

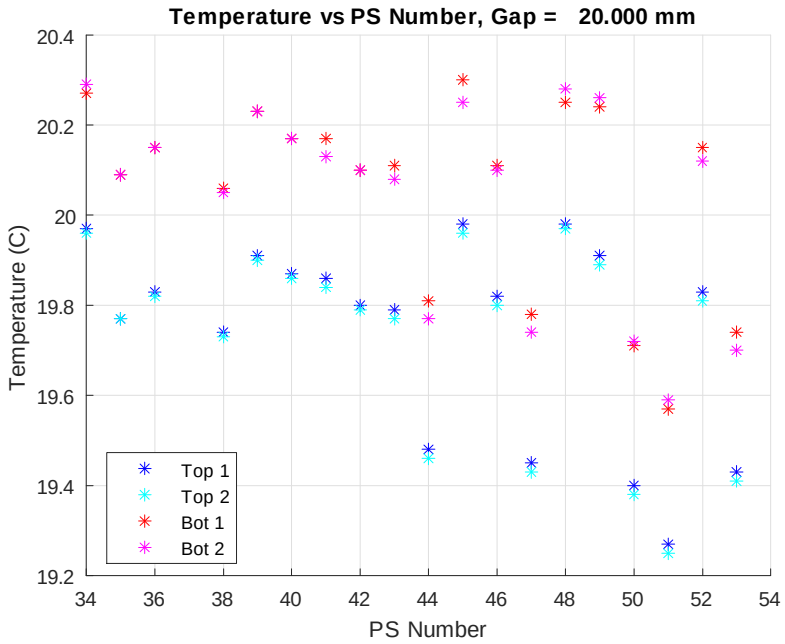

Figure 31: Temperature of the upper and lower jaws of the SXR phase shifters measured during their calibration.

12 Conclusion

A magnetic design was presented based on the LCLS-II phase shifters. The PPM design used magnet blocks with a remnant field of $B_r = 1.25$ T. The design meets the requirements on phase integral and fringe field length using a block length of 19 mm, a block height of 25 mm, and a block width of 65 mm. The phase shifter can do 10% energy scans without jumps. A prototype should be built to test the design as the next step in producing the LCLS-II-HE phase shifters.

Acknowledgements
Many thanks to Heinz-Dieter Nuhn for valuable discussions about this note.